The Geant4 Hadronic Verification Suite for the Cascade Energy Range

V. Ivanchenko
BINP, Novosibirsk, 630090, Russia and
CERN, Geneve, CH 1211, Switzerland
G. Folger, J.P. Wellisch
CERN, Geneve, CH 1211, Switzerland
T. Koi, D.H. Wright
SLAC, Stanford, CA 94025, USA

A Geant4 hadronic process verification suite has been designed to test and optimize Geant4 hadronic models in the cascade energy range. It focuses on quantities relevant to the LHC radiation environment and spallation source targets. The general structure of the suite is presented, including the user interface, stages of verification, management of experimental data, event generation, and comparison of results to data. Verification results for the newly released Binary cascade and Bertini cascade models are presented.

1. INTRODUCTION

The Geant4 toolkit [1] includes a collection of models and packages for hadronic physics which are applicable to various particle transport problems [2]. In Geant4, final state generation is separated from the access and use of cross sections and from tracking. It is therefore possible and desirable to have independent, alternative physics models. In order to optimize these models and to identify their most appropriate application, detailed comparisons between experimental data and model predictions are required.

The cascade energy region from the reaction threshold to incident hadron energies of a few GeV is problematic for all existing Monte Carlo packages. In order to verify and further develop Geant4 models in this energy range, a verification suite has been created. The stages of the verification, including experimental data handling, event generation and comparison to data are described here. Results of the comparison are also presented.

2. VERIFICATION SUITE

2.1. Method

The verification suite is generic, as it is based on an abstract interface to a final state hadronic interaction generator. This interface can be found in Level 2 of the Geant4 hadronic physics framework [3]. It focuses on quantities relevant to the LHC radiation environment and spallation source targets.

The modular structure of Geant4 allows the generation of single events with a known incident particle energy and an explicitly defined hadronic final state generator. The kinematics of secondaries produced in the interaction are analyzed and the resulting angular, momentum, energy, and baryon number spectra are stored in histograms. The energy-momentum balance can be controlled as well. The histograms are compared to published measurements of the differential and double differential cross sections, $d\sigma/dE$, $d\sigma/d\Omega$, $d^2\sigma/dEd\Omega$, and the invariant cross sections, $Ed^3\sigma/d^3p$.

The cross section contributing to the i-th bin of the histogram are given by

$$\Delta\sigma_i = \sigma_{tot}N_i/N, \qquad (1)$$

where σ_{tot} is the total cross section for the interaction being tested, N is the number of simulated events in the sample, and N_i is the number of times bin i is incremented during the run. Each bin represents a small region of phase space such as $\Delta\Omega$, ΔE, or $\Delta\Omega\Delta E$, into which the secondary particle goes after being produced in the interaction. The double differention cross section is estimatated as

$$\frac{d^2\sigma}{dEd\Omega} = \frac{\Delta\sigma_i}{\Delta E\Delta\Omega}. \qquad (2)$$

The verification suite is organized into a number of test cases, each defined by a unique incident beam energy and a single target nucleus. All data files, macro files, kumac files and results for each case are stored in a separate subdirectory. The AIDA abstract interface [4] is used in the suite for histogram creation and filling. The output is done in ASCII and HBOOK formats.

2.2. Cross Sections

The verification is done by comparing simulation results with experimental data mainly from the EXFOR database [5]. Only data with absolute measurements of the differential cross sections are utilized in the suite. The data downloaded from the database are re-formatted in order to provide intermediate files acceptable for PAW analysis. In some cases re-binning of the data was performed during this process. This was required mainly for the low energy part of the

Table I Neutron production by incident protons.

Target nucleus	Beam energy(MeV)
Be	113, 256, 585, 800
C	113, 256, 590
Al	22, 39, 90, 113, 160, 256, 585, 800
Fe	22, 65, 113, 256, 597, 800
Ni	585
Zr	22, 35, 50, 90, 120, 160, 256, 800
Pb	35, 65, 113, 120, 160, 256, 597, 800

Table II Pion production by incident protons.

Target nucleus	Beam energy(MeV)
H	585
D	585
Be	585
C	590
Al	585, 730, 1000
Cu	730
Ni	200, 585
Pb	585, 730

spectra. If, within a given test case, only double differential cross section data are available, the single differential cross sections are obtained by numerical integration.

Initial verifications have been performed for neutrons and pions produced by protons incident upon various targets. For these test cases the initial proton energies were all below 1 GeV. In this energy region the inclusive reaction channel

$$p + A \rightarrow n + X, \qquad (3)$$

has been studied experimentally for many years. The secondary neutrons can be identified and their energies can be measured with good precision by using time-of-light techniques. Because this reaction is important for many applications, a significant number of test cases have been created for it (Table I).

For HEP applications and in particular for the LHC detector, simulating secondary pion production is important. Model verification for pion production by incident protons is available for several test cases (Table II) for the reactions

$$p + A \rightarrow \pi^{\pm} + X. \qquad (4)$$

2.3. User Interface

The user interface is implemented by macro files which allow the specification of various parameters of the verification. These include:

- initial particle and its energy,
- beam energy spread,
- target nucleus,
- hadronic interaction generator,
- generator options, and
- histogram types and bins.

Both linear and logarithmic binning are available. Each verification test case contains a script which executes the macro files. Hence the user can perform the complete verification process by issuing a single command. The results are stored in HBOOK format and can be processed in PAW by prepared kumac files.

3. HADRONIC MODELS

The verification suite has been used extensively during the release phase of the new Geant4 Bertini cascade and Binary cascade packages [2]. The Bertini cascade model is a classical cascade code which was described in detail at another presentation at this conference [6].

The Binary cascade introduces a new approach to cascade calculations. The interaction is modeled exclusively on binary scattering between reaction participants and nucleons. The nucleus is described by a detailed 3-dimensional model in which the nucleons are explicitly positioned in phase space. Free hadron-hadron elastic and reaction cross sections are used to define the collisions. Propagation of the particles in the nuclear field is done by numerically solving the the equation of motion.

The cascade begins with a projectile and a description of the nucleus, and terminates when the both average and maximum energy of all particles within the nuclear boundary are below a given threshold. The remaining nuclear fragment is treated by pre-equilibrium decay and de-excitation models [7].

4. RESULTS OF VERIFICATION

4.1. Inclusive neutron spectra

The single and the double differential inclusive neutron spectra are very sensitive to the physics model used in the cascade code. As shown in Fig. 1, the Binary cascade reproduces the data rather well for all targets, except for energies below 50 MeV where neutron evaporation is important. In contrast, the Bertini cascade (Fig.2) does well below 50 MeV for all but the lightest nuclei. Above 50 MeV only the general trend of the data is reproduced, while the overall normalization improves as A increases.
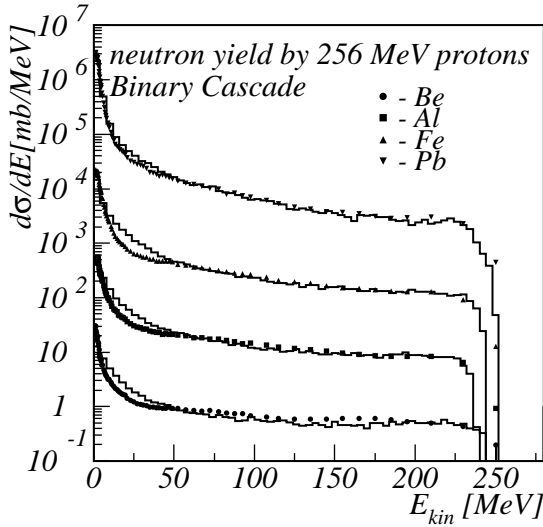
Figure 1: Neutron yield produced by 256 MeV protons. Histograms - Binary Cascade predictions, points - data [9].
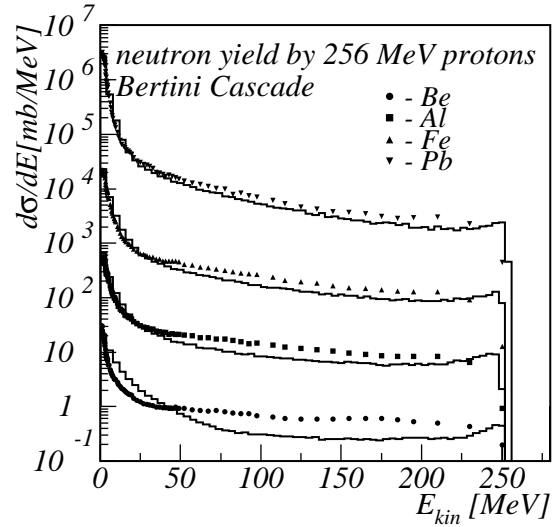

Figure 2: Neutron yield produced by 256 MeV protons. Histograms - Bertini Cascade predictions, points - data [9].

Fig. 3 shows forward scattering in which the proton transfers its energy to one target neutron. Here the Binary cascade describes the data above 50 MeV. The Bertini cascade (Figs.4) does less well, significantly underestimating the data at higher neutron energies. This discrepancy is reduced for heavier nuclei.

Additional verification test cases indicate that the Binary cascade approach is reasonably accurate for other angles and energies as well. Fig. 5 shows comparisons for aluminum at forward and backward neutron angles at energies of 113, 256, 585 and 800 MeV. At 113 and 256 MeV, agreement at all angles is good. At 585 and 800 MeV the backward angle spectra are not well-reproduced. The same set of plots is shown in Fig. 6 for iron, and in Fig. 7 for lead. For both targets the same trends apply as were observed in aluminum.

4.2. Pion production

Another useful test of the cascade codes is to look at the double differential cross sections for the production of π^+ and π^-. Experimental cross sections show that π^+ production by protons is significantly larger than that for π^-. This feature is well-reproduced by the Binary cascade as shown in Fig.8. The trend of the cross section versus energy is also reproduced, although the overall normalization is underestimated by a factor of 2-3 for carbon, aluminum and nickel.

Similar plots for π^+ and π^- are shown for an incident proton energy of 730 MeV. Figs.9 and 10 show π^- and π^+ at forward and backward angles from aluminum, while Figs. 11 and 12 show π^- and π^+ from copper. In all these cases the observed ratio of π^+ to π^- production is reproduced. As was the case for 597 MeV incident protons (Fig. 8), the trend of cross
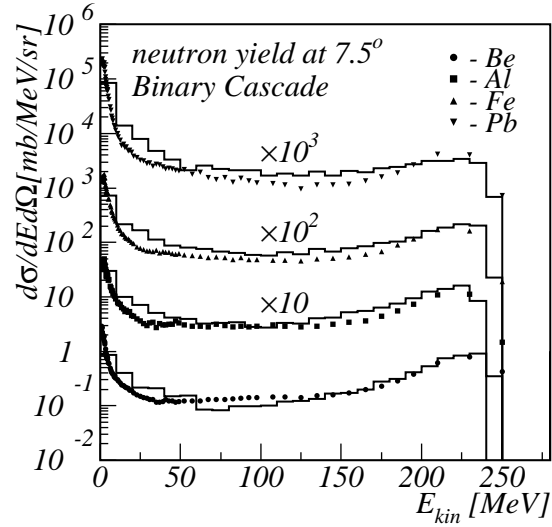

Figure 3: Double differential cross-section for neutrons produced at 7.5 degrees by 256 MeV protons. Histograms - Binary Cascade predictions, points - data [9].

section versus energy is also reproduced. However at 730 MeV it is seen that the Binary cascade does an increasingly poor job of reproducing the overall normalization as the pion angle increases.

4.3. Future verification work

While the existing verification suite has already been used extensively, further development is required. So far the validity of the cascade codes has only been demonstrated for incident protons at the low end of their energy ranges. In order to test the full range of energies and particles, many more test
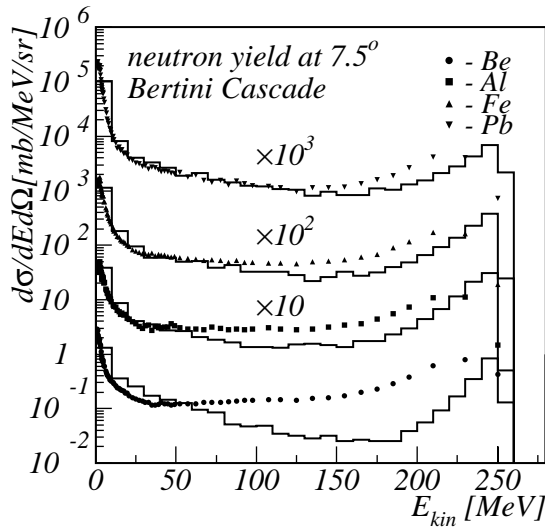
Figure 4: Double differential cross-section for neutrons produced at 7.5 degrees by 256 MeV protons. Histograms - Bertini Cascade predictions, points - data [9].

cases are required, including:

- incident proton energies up to 15 GeV,

- incident pion energies up to 15 GeV.

- incident neutrons, and

- proton inclusive spectra.

5. CONCLUSIONS

A verification suite for hadronic interaction models in the cascade energy region has been designed and implemented. This suite has been used both to develop the Bertini and Binary cascade model codes for the Geant4 toolkit and to compare their predictions with data from thin target scattering experiments.

The suite has proved to be an efficient tool for model validation which can be used for the development and testing of other hadronic interaction models. The suite is also being expanded to include tests for more types of incident particles and higher energies.

Acknowledgments

References

[1] GEANT4 (S. Agostinelli et al.), GEANT4: A Simulation Toolkit, SLAC-PUB-9350, Aug 2002. 86pp. Will be published in *Nucl. Instrum. Meth. A*.

[2] J. P. Wellisch, Geant4 hadronic physics status and validation for large HEP detectors. Talk at this conference MOMT002.

[3] J. P. Wellisch, Hadronic shower models in Geant4 - the frameworks, Comp. Phys. Comm. 140 (2001) 65-75.

[4] AIDA – Abstract Interfaces for Data Analysis. http://aida.freehep.org/

[5] EXFOR database. http://www.nea.fr/html/dbdata/

[6] A. Heikinen, N. Stepanov, and J. P. Wellisch, Bertini intra-nuclear cascade model implementation in Geant4. Talk at this conference MOMT008.

[7] V. Lara and J. P. Wellisch, Pre-equilibrium and equilibrium decays in GEANT4, Proceedings of Computing in high energy and nuclear physics CHEP2000 Padova, page 52.

[8] M. M. Meier et al., Differential neutron production cross sections and neutron yields from stopping-length targets for 113-MeV protons, Nucl. Scien. Engin. **102**, 310, (1989)

[9] M. M. Meier et al., Differential neutron production cross sections for 256-MeV protons, Nucl. Scien. Engin. **110**, 289, (1992)

[10] W. B. Amian et al., Differential neutron production cross sections for 597-MeV protons, Nucl. Scien. Engin. **115**, 1, (1993)

[11] W. B. Amian et al., Differential neutron production cross sections for 800-MeV protons, Nucl. Scien. Engin. **112**, 78, (1992)

[12] J. F. Crawford et al., Measurement of cross sections and asymmetry parameters for the production of charged pions from various nuclei by 585-MeV protons, Phys. Rev. **C 22**, 1184, (1980)

[13] D. R. F. Cochran et al., Production of changed pions by 730-MeV protons from hydrogen and selected nuclei. Phys. Rev. **D6**, 3085 (1972).
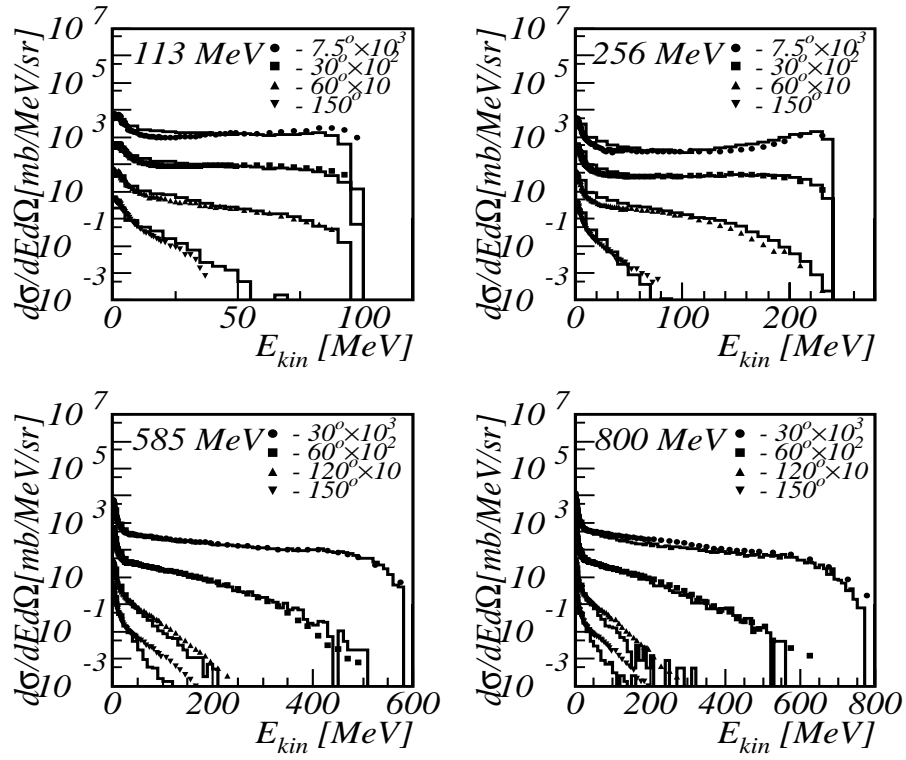
Figure 5: Double differential cross-section for neutrons produced in proton scattering off aluminum. Histograms - Binary Cascade predictions, points - data [8, 9, 10, 11].
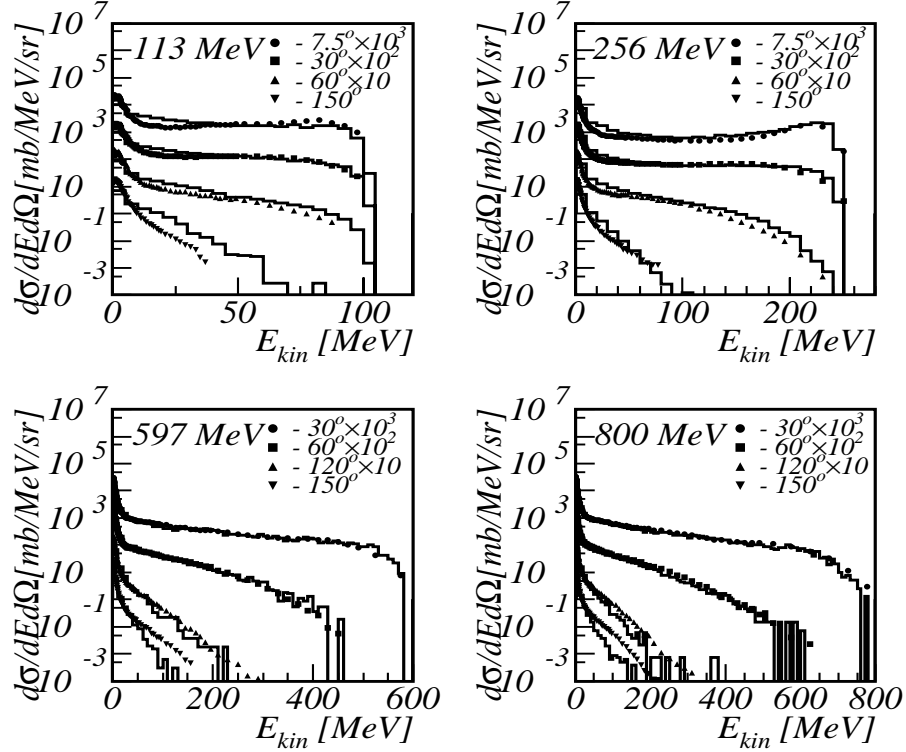

Figure 6: Double differential cross-section for neutrons produced in proton scattering off iron. Histograms - Binary Cascade predictions, points - data [8, 9, 10, 11].
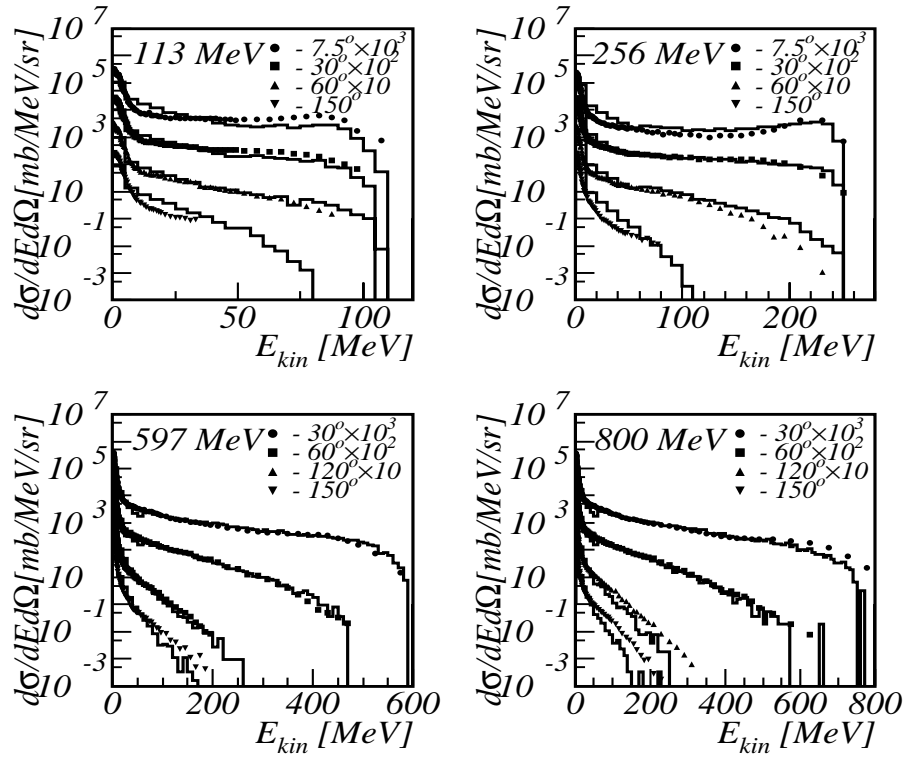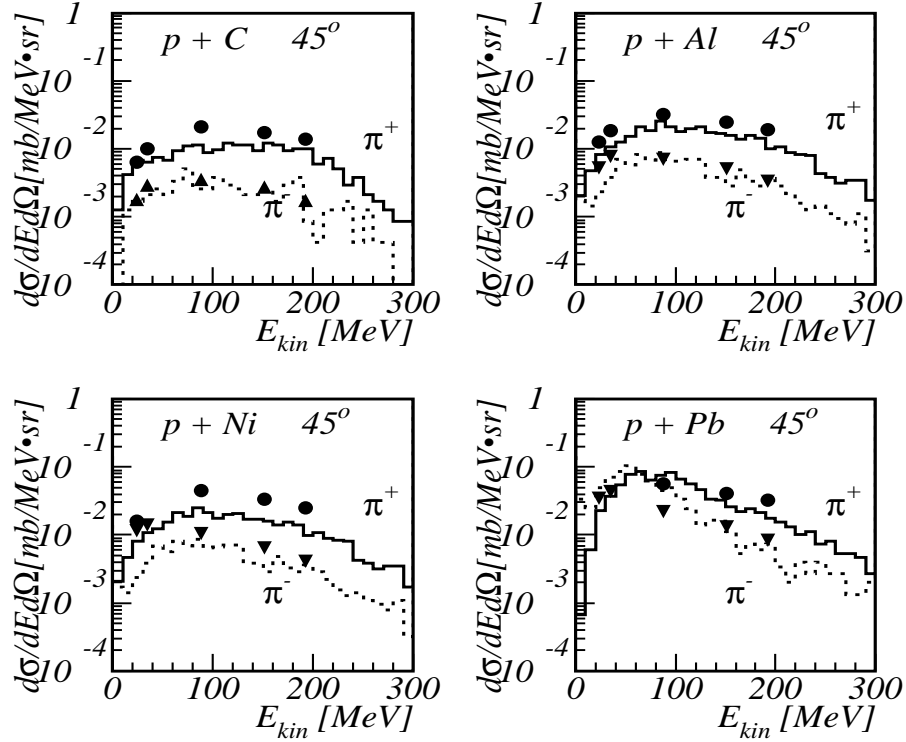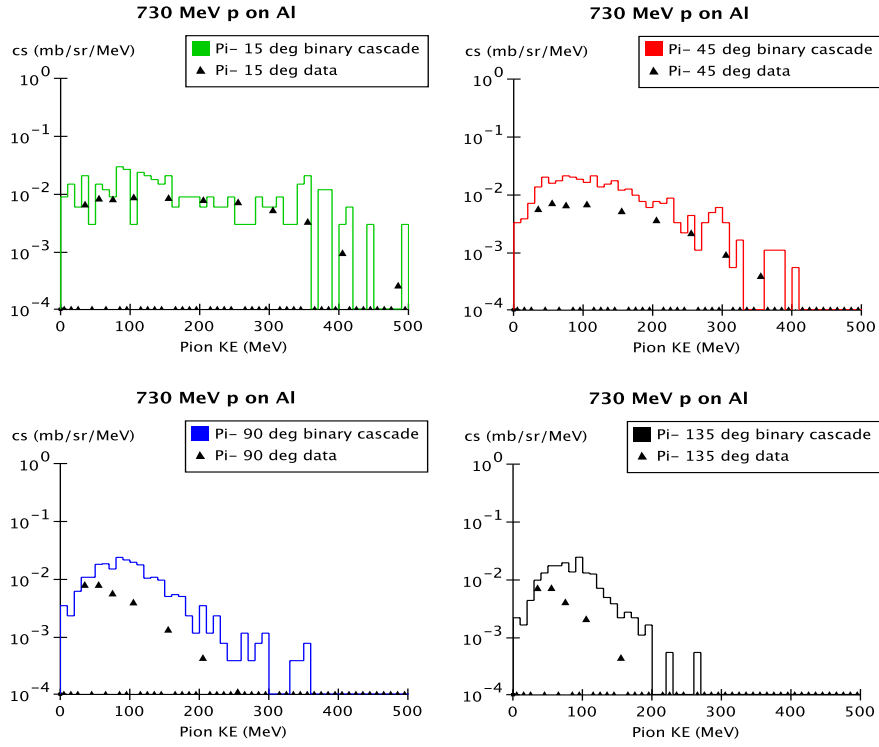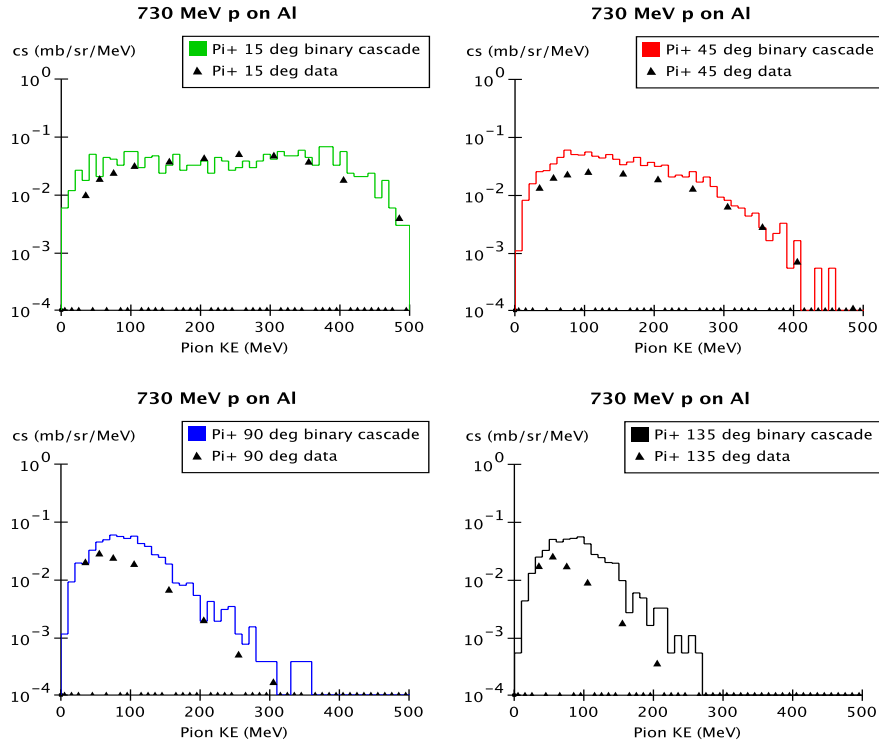
Figure 7: Double differential cross-section for neutrons produced in proton scattering off lead. Histograms - Binary Cascade predictions, points - data [8, 9, 10, 11].

Figure 8: Double differential cross-section for pions produced at 45° in 597 MeV proton scattering off various materials. Histograms - Binary Cascade predictions, points - data [12].

Figure 9: Double differential cross-section for π^- produced in 730 MeV proton scattering off aluminum. Histograms - Binary Cascade predictions, points - data [13].

Figure 10: Double differential cross-section for π^+ produced in 730 MeV proton scattering off aluminum. Histograms - Binary Cascade predictions, points - data [13].
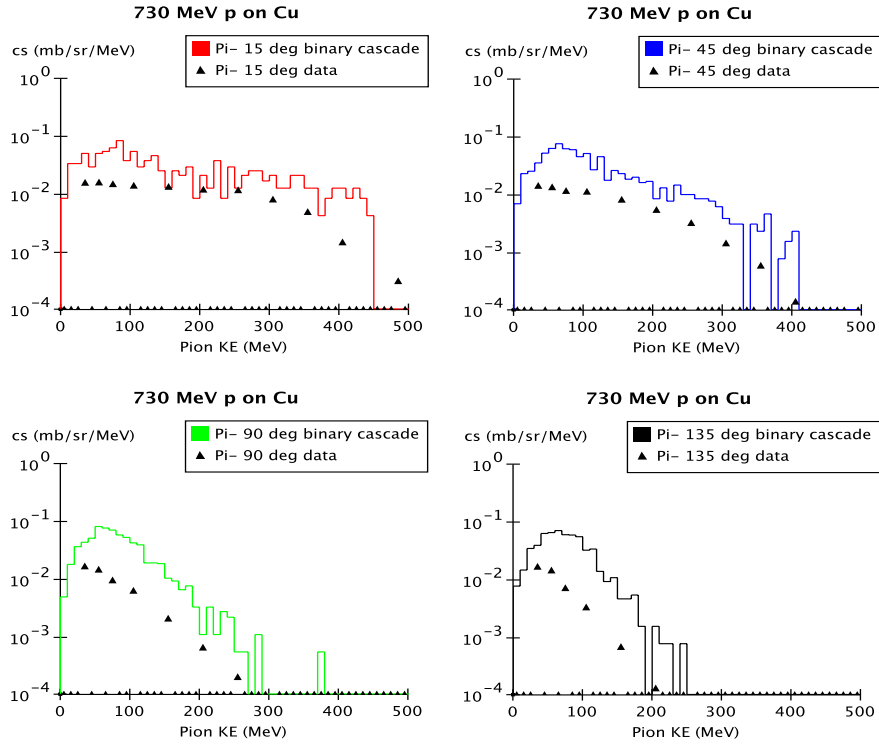
Figure 11: Double differential cross-section for π^- produced in 730 MeV proton scattering off copper. Histograms - Binary Cascade predictions, points - data [13].
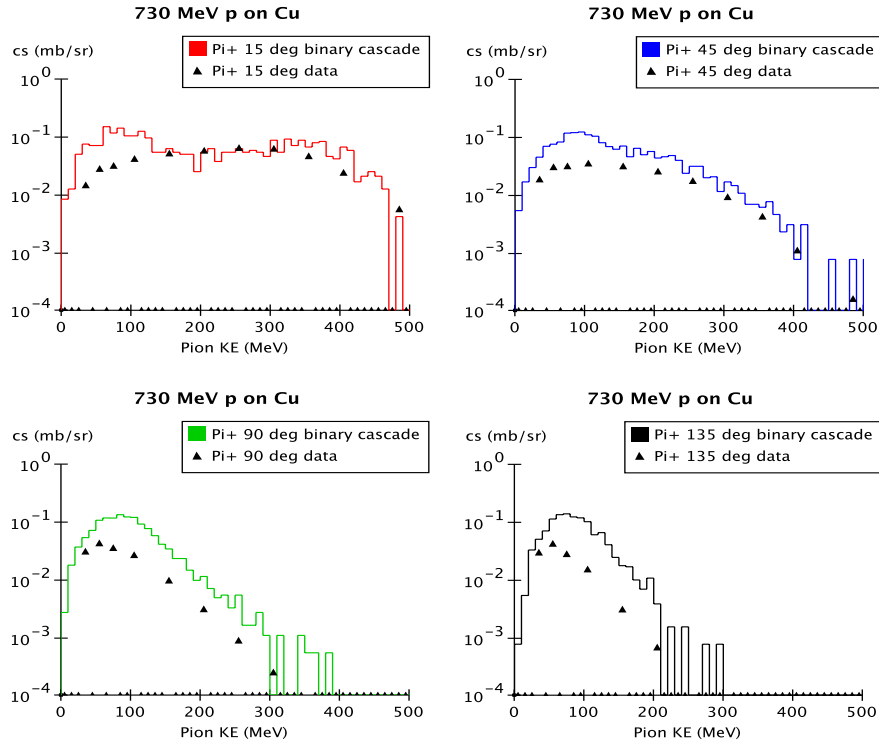

Figure 12: Double differential cross-section for π^+ produced in 730 MeV proton scattering off copper. Histograms - Binary Cascade predictions, points - data [13].
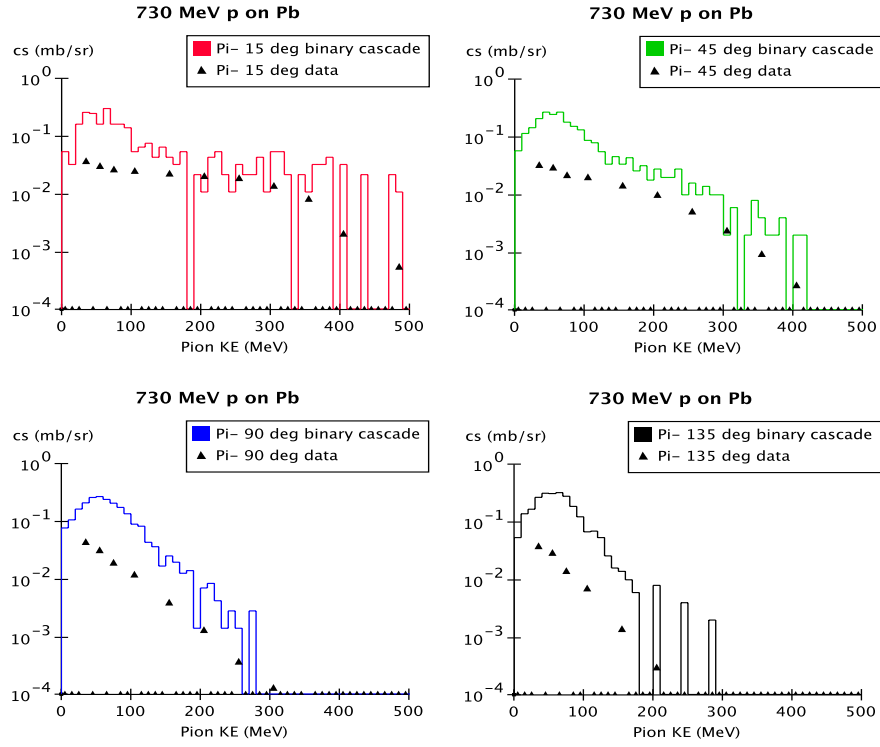
Figure 13: Double differential cross-section for π^- produced in 730 MeV proton scattering off aluminum. Histograms - Binary Cascade predictions, points - data [13].
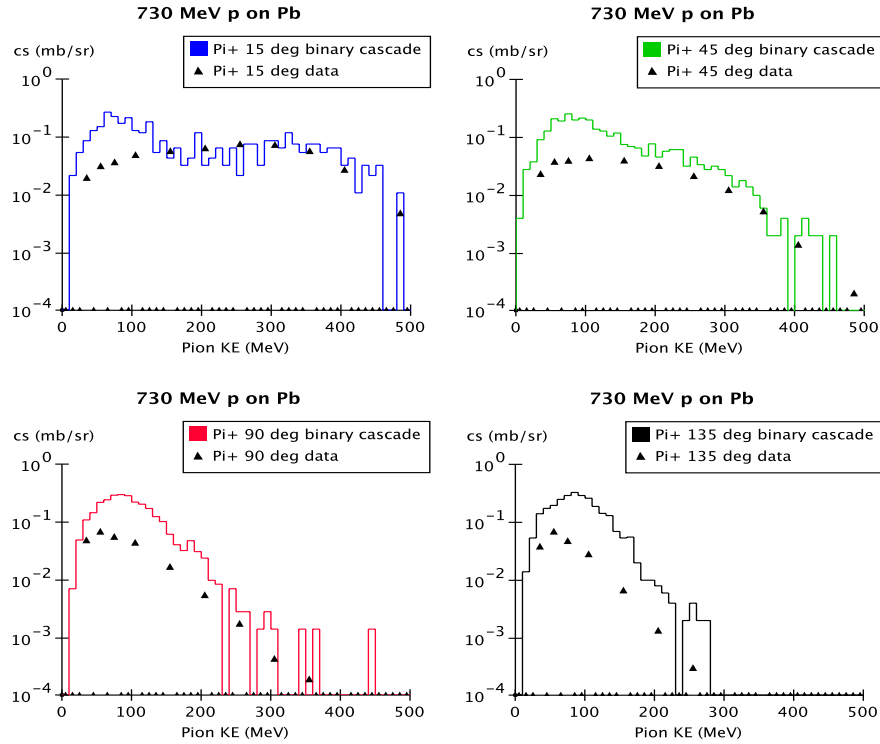

Figure 14: Double differential cross-section for π^+ produced in 730 MeV proton scattering off aluminum. Histograms - Binary Cascade predictions, points - data [13].